Microscopic observation of chemical modification in sections using scanning acoustic microscopy

Pathology International
OFFICIAL JOURNAL OF THE JAPANESE SOCIETY OF PATHOLOGY

Microscopic observation of chemical modification in sections using scanning acoustic microscopy

Journal:	*Pathology International*
Manuscript ID:	PIN-2014-00156.R1
Manuscript Type:	Original Article
Date Submitted by the Author:	14-Jan-2015
Complete List of Authors:	Miura, Katsutoshi; Hamamatsu University School of medicine, Pathology Egawa, Yuki; Shizuoka City Shizuoka Hospital, Diagnostic Pathology Moriki, Toshiaki; Shizuoka City Shizuoka Hospital, Diagnostic Pathology Mineta, Hiroyuki; Hamamatsu University School of Medicine, Department of Otorhinolaryngology Harada, Hidekazu; Hamamatsu University Hospital, Division of Pathology Baba, Satoshi; Hamamatsu University Hospital, Division of Pathology Yamamoto, Seiji; Hamamatsu University School of Medicine, Medical Photonics Research Center
Key Words:	aging, imaging analysis, elasticity, formalin fixation, histochemistry, histopathology, ultrasound, pepsin, periodic acid-Schiff reaction

Microscopic observation of chemical modification in sections using scanning acoustic microscopy

Katsutoshi Miura[1], Yuki Egawa[2], Toshiaki Moriki[2], Hiroyuki Mineta[3], Hidekazu Harada[4], Satoshi Baba[4], and Seiji Yamamoto[5]

[1]Department of Health Science, Pathology and Anatomy, Hamamatsu University School of Medicine, Hamamatsu, Japan

[2]Department of Diagnostic Pathology, Shizuoka City Shizuoka Hospital, Shizuoka, Japan

[3]Department of Otorhinolaryngology, Hamamatsu University School of Medicine, Hamamatsu, Japan

[4]Division of Pathology, Hamamatsu University Hospital, Hamamatsu, Japan

[5]Medical Photonics Research Center, Hamamatsu University School of Medicine, Hamamatsu, Japan

Correspondence:

Katsutoshi Miura, MD, PhD

Department of Health Science, Pathology and Anatomy,

Hamamatsu University School of Medicine,

1-20-1 Handayama, Higashi-ku,

Hamamatsu 431-3192, Japan

Tel/Fax: +81 53 435 2800

Email: kmiura@hama-med.ac.jp

Running title: Ultrasound detection of tissue modification

Conflict of interest: Nothing to declare in terms of conflict of interest and funding

Abstract

A scanning acoustic microscope (SAM) calculates the speed of sound (SOS) through tissues and plots the data on the screen to form images. Hard tissues result in greater SOS; based on these differences in tissue properties regarding SOS, SAM can provide data on tissue elasticity. The present study evaluated whether tissue modifications, such as formalin fixation, periodic acid-Schiff (PAS) reactions and protein degradation, changed the acoustic properties of the tissues and whether SAM could be a useful tool for following chemical changes in sections. The fixation process was observable by the increased SOS. During the PAS reaction, the glycosylation of tissues was characterized by an increased SOS. Mucous or glycogen distribution was visualised and was found to be statistically comparable among lesions and states. Protease digestion by pepsin led to a decreased SOS. Tissue sensitivity to proteases varied due to the stage, cause and duration of inflammation or ageing. Changes in acoustic properties were more sensitive than those in optical histology. SAM facilitates the visualisation of the time course or distribution of chemical modifications in tissue sections, thus aiding their comparison among tissues. SAM may be an effective tool for studying changes such as protein cross-linkage, tissue repair and ageing.

Keywords: ageing; elasticity; formalin fixation; histochemistry; histopathology; imaging analysis; pepsin; periodic acid-Schiff reaction; ultrasound

INTRODUCTION

Chemical changes in tissues are often accompanied by subtle morphological changes that may not be visible with conventional light microscopy (LM). LM requires special stains with specific dyes and antibodies that have a high affinity for specific structures and ligands. These methods require extra time, extra costs and special techniques. Moreover, the repeated observation of the same slides before and after chemical reactions may be difficult. A scanning acoustic microscope (SAM) can observe the acoustic properties of tissue sections without special stains [1]. It may be easier to follow the microscopic changes that occur due to modifying conditions and over time on the same section with SAM than with LM. SAM calculates the speed of sound (SOS) through tissues and plots the data on the screen to form images. Hard tissues result in greater SOS; based on these differences in tissue properties regarding SOS, SAM can provide data on tissue elasticity as well [3]. If a chemical modification induces an alteration of the acoustic properties of the tissue and affects tissue elasticity, SAM can visualise the modified areas in the section without the requirement of any auxiliary techniques.

Here, we have shown the results of SAM observations following chemical

modifications in tissue sections that had been treated with formalin fixation, periodic acid-Schiff (PAS) reactions or proteinase digestion.

MATERIALS AND METHODS

Materials and Ethics

All human sections were prepared from the Hamamatsu University Hospital archives. The research protocol for using stored samples without a link to patient identity was approved by the Ethics Committee of Hamamatsu University School of Medicine. Written consent was obtained from the family of the deceased for autopsy cases and was waived by all living patients for inclusion in the retrospective study. Animal sections were prepared from three mice for each experiment, All animal research protocols were approved by the local Institutional Care and Animal Use Committee. For fresh frozen tissues, snap-frozen sections were cut to 10-μm thickness and stored in the freezer before use. Formalin-fixed, paraffin-embedded (FFPE) blocks were also flat-sectioned into slices of 10-μm thickness. Deparaffinized, unstained sections were soaked in distilled water for at least 3 h before observation to reduce hydrophobicity.

Observation with SAM

The SAM (AMS-50AI) was supplied by Honda Electronics (Toyohashi, Aichi, Japan) and was equipped with a 120-MHz or 400-MHz transducer. The SAM used ultrasound to image an object by plotting the SOS through the sections on screen [2]. We recently

reported that SAM could identify various tissues and lesions, such as the lung [4], stomach [5], thyroid [6] and lymph nodes [7].

The region of interest for acoustic microscopy was determined from the LM images. The SOS for the 300 × 300 points was calculated and plotted on the screen to create the images, and sound data from 64 cross points on the lattice screen were used for the statistical analysis.

Statistical analysis

The data regarding the SOS from each tissue element are provided as mean ± standard deviation (SD; m/s). The student's *t*-test was used for determining statistical differences among specimens.

Formalin fixation

Fresh frozen sections were soaked in 10% buffered formalin, removed, washed in distilled water and then observed under SAM. The soaking time for the tissue sections was subsequently extended from 3 min to 24 h.

To investigate the effect of formalin fixation, we compared the images of cells between ethanol and formalin fixation. Oral squamous cells and peripheral white blood

cells were smeared on the glass slides and fixed in 95% ethanol for 30 min. After washing in distilled water, the slides were observed under SAM. Then, the cells were fixed in 10% formalin for 10 min, and the same areas were re-observed under SAM.

To determine the effects of fixation duration on paraffin sections, various organs of mice such as the heart, large intestine, liver and kidney were soaked for different fixation times: 1 day, 1 week and 3 months. The acoustic images of the FFPE tissues were compared in each organ.

Periodic acid-Schiff reaction

The fresh frozen and deparaffinized sections were soaked in distilled water and oxidized in 1% periodic acid solution for 10 min. The sections were rinsed in distilled water for 7 min and mounted with Schiff reagent for 10 min. Before the reaction, after the periodic acid oxidation and after the Schiff reagent, the sections were washed in distilled water and observed with SAM.

Protease digestion

The paraffin sections were dewaxed in xylene, soaked in distilled water and digested

in pepsin (Sigma P-6887, St.Louis, MO, USA) solution (12 units/mL in 10 mM HCl) at 37 °C for 1 and 3 h. The sections were washed in distilled water and observed under SAM. The same sections were used for repeated digestion.

Light microscopic observation

To compare the SAM images of the LM images, the same or nearby sections were stained with HE or Elastica–Masson staining.

RESULTS

SOS after formalin fixation

The SOS through fresh intestines increased according to the duration of fixation time (Fig. 1A-B, Table S1) and the concentration of formalin. Compared with ethanol fixation, formalin fixation induced a greater SOS through tissues and reduced the thickness of the tissues (Fig. 2A-C, Table S2-3).

However, the FFPE tissue sections of each organ demonstrated stable values for SOS at different fixation periods (Fig. 3A-B, Table S4). No significant difference was found ($P < 0.05$).

Periodic acid-Schiff reaction

After the periodic acid oxidation, the fresh frozen colon tissue displayed increased SOS at the mucosal mucin of the goblet cells as dots (Fig. 4A). No optical changes were found in this process. After treatment with the Schiff reagent, the dots spread over the entire mucosa and increased in size and number. On the paraffin sections of the kidney, the SOS increased for the basement membranes of the glomeruli and tubules after the periodic acid-Schiff (PAS) reaction (Fig. 4B-C). Compared with the normal kidney, the

diabetic kidney displayed a remarkable increase in SOS at the sclerotic glomeruli and thickened basement membranes. Both values were significantly elevated after the PAS reaction ($P < 0.01$) in the diabetic kidney (Fig. 4D, Table S5). The more glycosylated portions displayed a higher SOS.

Protease digestion

The FFPE sections of the mouse ulcerated skin displayed a rapid decrease in the SOS after pepsin digestion (Fig. 5A). The epidermal keratins, dermal fine collagen fibres of granulation tissue and skeletal muscle fibres were more sensitive to protease digestion, while the thick collagen fibres in the deep dermis revealed greater resistance (Fig. 5B, Table S6). By LM using Elastica–Masson or HE staining, the histological structures were well preserved.

The layered structures of the aortic valve from a 53-year-old patient were destroyed or almost disappeared after treatment with pepsin (Fig. 6A). The values of the average SOS between predigestion and 1 h after digestion and between 1 h and 3 h after digestion were significantly different (Fig. 6C, Table S7). Under LM, after staining of the same valve after digestion, the aortic valve retained its original structures, although

the collagenous or elastic fibres became paler.

Compared with the valve of a younger person, the valve of an elderly person displayed resistance to protease digestion after being subjected to the same incubation conditions. During the process of pepsin digestion, the aortic valve of a 74-year-old male demonstrated almost the same SOS values (Fig. 6B), although the ventricularis layer consisting of the fine elastic fibres showed only a slight reduction in SOS. No significant differences in SOS were found among the different incubation periods (Fig. 6C, Table S7). With LM staining, the valves maintained their structures well enough to maintain their original layers.

To demonstrate the utility of this technique in the evaluation of the interval after myocardial infarction, areas of old and fresh infarction were assayed and shown to demonstrate different SOS values after protease digestion. The areas of old infarction with fibrous scars demonstrated protease-resistance 1 h after digestion (Fig. 7A), while those of early infarction consisting of haemorrhagic necrosis and neutrophillic infiltration showed a rapid decrease in SOS (Fig. 7B). The reduction of SOS values from before digestion to 1 h after digestion, and also from 1 h to 3 h after digestion was

significant ($P < 0.01$) (Fig. 7C, Table S8). Normal cardiac muscles also showed a significant decrease in SOS after pepsin digestion.

DISCUSSION

Formalin fixation created cross-links among proteins such as arginine, lysine, serine and tyrosine amino acid residues [8] and made tissues firmer than fresh tissues. Evaluating the firmness of tissues is objectively impossible using only LM. SAM can visualise tissue hardness by plotting the SOS through tissues because harder tissues exhibit a higher SOS. The digital data obtained with SAM can be compared statistically between different tissues and lesions. After formalin fixation, these values increased in proportion to the formalin concentration and the duration of fixation time as seen in Fig. 1A-B. The reasons for the increase in SOS value with formalin fixation are not only the cross-links but the decrease in tissue thickness as seen Fig. 2A-C. Protein cross-links may reduce and compact the cells, which results in increasing their hardness.

FFPE tissues showed stable SOS values independent of the fixation period, which means that the FFPE tissues had the same hardness. After formalin fixation, heating and dehydration by organic solvent were performed to make paraffin blocks. The complex processing of the FFPE sections may cause stable firmness, and these properties are beneficial for the comparison of SOS among the same FFPE organs.

During the PAS reaction, glycosylated portions of the fresh tissues showed a small increase in SOS after periodic acid oxidation while no optical changes were seen. After treatment with the Schiff reagent, a more conspicuous increase in SOS was found. The portions that were more glycosylated such as the diabetic glomeruli and tubular basement membrane displayed a greater SOS and corresponded well to the PAS-positive areas on LM histology. Comparing the degree of diabetic glycosylation can be difficult by LM observation, but is possible with SAM using numerical analysis as seen Fig. 4D. It means that degree of glycosylation is calculable and comparable by SOS values. SAM will also be a useful tool to study the histological changes of ageing because advanced glycation end products increase with age [9].

Proteases break down structural proteins such as collagen and elastic fibres. As detailed on the manufacturer's product sheet, pepsin was made from porcine gastric mucosa and can break down the peptide bonds of universal proteins. From the above experiment, the optical histology after pepsin digestion still retained the original structures. On the contrary, the ultrasonic properties were quite sensitive to protease digestion, and SAM could quantitatively detect the subtle structural changes based on the SOS through the section. Moreover, SAM offered the advantage of the ability to use

the same section with no special staining. As such, the same section can be monitored by changing the incubation time and reaction conditions.

After protease digestion, SAM can be used to evaluate the development of fibrosis. Fibrosis is a consequence of inflammation, ischaemia, cancer invasion and other pathological events [10,11]. Myofibroblasts produce collagen fibres that undergo chemical modifications such as glycation and bridging, and the degree of modification varies among tissues or among ages [12]. Younger collagen fibres without modification, which may appear in granulation tissues after infarction or inflammation, the dermis of young patients and intact cardiac valves, were vulnerable to protease digestion. However, old fibrotic tissues, such as old infarctions, repeated inflammations or scar tissue and degenerated cardiac valves, exhibited resistance to protease breakdown because the chemical modifications interfered with the protease activities.

The results of the protease digestion revealed that the alteration in the SOS before and after the treatment differed among tissues and by age and duration of inflammation, which corresponded well with the expected results above. Numerical analysis of the ultrasonic properties that reflected the sensitivity or resistance to protease digestion may

be useful for estimating the age and degree of modification from fibrosis. This information may be useful for studying tissue repair processes and tissue ageing.

Proteases with a particular substrate specificity such as collagenase or elastase may show the distribution and amount of the specific structural protein. Stripping by specific enzymes and observing with SAM may be a useful tool for studying the histological structures of organs.

Today, proteomic analysis, which is the global analysis of protein expression in cells and tissues, may be possible from FFPE tissues [13]. To purify the proteins from them, protease digestion is necessary. To evaluate the possibility or success of protein extraction from the sections, SAM may provide more useful information than LM.

In conclusion, SAM facilitates the visualisation of the time course or distribution of chemical modifications on sections and makes it possible to statistically compare the degree of chemical changes among tissues. Changes in acoustic properties in protease digestion are more sensitive than those of optical histology. SAM may be effective for studying histological changes, such as protein cross-linkage, glycosylation, structural

proteins, tissue repair and ageing.

Acknowledgments

We thank K. Kobayashi (Honda Electronics Co., Ltd., Toyohashi, Japan) for his technical support and advice on scanning acoustic microscopy and Y. Kawabata, N. Suzuki and K. Sugaya for preparing the tissue sections. The authors would like to thank Enago (www.enago.jp) and Wiley Editing Services for the English language review.

Disclosure

This work was supported by a Japan Society for the Promotion of Science KAKENHI, Grant Number Scientific Research (c) 24590445.

Each author's contribution

Katsutoshi Miura observe the slides, collected data, and prepared the paper. Yuki Egawa, Toshiaki Moriki, Hiroyuki Mineta, and Hidekazu Harada prepared the samples for histochemical modifications. Satoshi Baba collected the clinical data from the records. Seiji Yamamoto set the SAM machine and helped to prepare the manuscript.

REFERENCES

1. Saijo Y. Acoustic microscopy: latest developments and applications. *Imaging Med* 2009; **1:** 47–63.

2. Miura K, Yamamoto S. Histological imaging from speed-of-sound through tissues by scanning acoustic microscopy (SAM). *Protocol Exchange* 2013; doi:10.1038/protex.2013.040

3. Wells PNT. Biomedical ultrasonics. Academic Press: London, 1977; 110–137.

4. Miura K, Yamamoto S. Pulmonary imaging with a scanning acoustic microscope discriminates speed-of-sound and shows structural characteristics of disease. *Lab Invest* 2012; **92:** 1760–1765.

5. Miura K, Yamamoto S. Histological imaging of gastric tumours by scanning acoustic microscope. *BJAST* 2014; **4:** 1–17.

6. Miura K, Mineta H. Histological evaluation of thyroid lesions using a scanning acoustic microscope. *Pathology and Laboratory Medicine International* 2014; **6:** 1–9.

7. Miura K, Nasu H, Yamamoto S. Scanning acoustic microscopy for characterization of neoplastic and inflammatory lesions of lymph nodes. *Sci Rep* 2013; **3:** 1255.

8. Hood BL, Conrads TP, Veenstra TD. Mass spectrometric analysis of

formalin-fixed paraffin-embedded tissue: unlocking the proteome within. *Proteomics* 2006; **6:** 4106–4114.

9. Bucala R. Diabetes, ageing, and their tissue complications. *J Clin Invest* 2014; **124:** 1887–1888.

10. White ES, Mantovani AR. Inflammation, wound repair, and fibrosis: reassessing the spectrum of tissue injury and resolution. *J Pathol* 2013; **229:** 141–144.

11. Ariel A, Timor O. Hanging in the balance: endogenous anti-inflammatory mechanisms in tissue repair and fibrosis. *J Pathol* 2013; **229:** 250–263.

12. Kapetanaki MG, Mora AL, Rojas M. Influence of age on wound healing and fibrosis. *J Pathol* 2013; **229:** 310–322.

13. Vincenti DC, Murray GI. The proteomics of formalin-fixed wax-embedded tissue. *Clin Biochem* 2013; **46:** 546–551.

Figure legends

Figure 1

Change in speed of sound after formalin fixation.

(A) A fresh frozen section of mouse small intestine was soaked in 10% buffered formalin for 3 min, washed in distilled water and observed under a scanning acoustic microscope (SAM). The same section was fixed according to the same process, but for varying durations of 1, 12 and 24 h. The values of speed of sound (SOS) increased in accordance with fixation time. The corresponding HE section after 24 h fixation is shown at the lower right.

(B) Average SOS (m/s) and SD of the mucosa after formalin fixation. $^{**}P < 0.01$, $^{*}P < 0.05$

Figure 2

Effects of fixation difference between ethanol and formalin.

Oral squamous cells (A) and peripheral white blood cells (B) were smeared on a glass slide, fixed in ethanol and observed with SAM. The cells were then fixed in 10% formalin. The upper figures indicate the SOS images and the lower figures indicate the thickness of each point. Each left and right image corresponds to almost same area. The

graph (C) shows average SOS (m/s) and thickness (μm) with SD. $^{**}P < 0.01$

Figure 3

The SOS of formalin-fixed, paraffin-embedded tissues at different fixation times.

(A) Images of SOS of various organs of mice such as heart, large intestines, liver and kidneys in different fixation times of 1 day, 1 week and 3 months are displayed.

(B) Average SOS (m/s) of various formalin-fixed, paraffin-embedded (FFPE) organs at different fixation times.

Figure 4

Change in SOS during the periodic acid Schiff procedure.

A fresh frozen section of mouse large intestine (A) was mounted with 1% periodic acid solution for 10 min, washed in distilled water and treated with Schiff reagent for 10 min. The images of SOS (left, before reaction; middle, after periodic acid oxidation; right, after Schiff reagent). The mucus in the goblet cells was pursuable by the increased SOS during the periodic acid Schiff (PAS) procedure. The corresponding light microscopic image after the PAS procedure is present at the lower right corner.

The SOS images of normal (B) and diabetic (C) kidney paraffin sections before and after PAS procedure. The SOS of the glomeruli and tubular basement membranes of the diabetic kidney promptly increased after the Schiff reaction compared with normal kidneys. The corresponding LM images are shown at the lower right corner. The graph (D) shows the average SOS (m/s) and SD of the glomeruli and tubules of normal and diabetic kidneys. Nor, normal; GM, glomerulus; T-BM, tubular basement membrane. $^{**}P < 0.01$

Figure 5

Change in SOS of mouse skin after pepsin digestion.

(A) A paraffin section of ulcerated mouse skin was incubated in pepsin in 10 mM HCl solution. After 1 and 3 h, the same section was observed under SAM. The epidermis, papillary dermis (PD) with granulation tissue and skeletal muscles (MS) displayed prompt reductions in SOS. The keratin fibres, fine collagen fibres and muscle fibres were more sensitive to protease digestion, while the thick collagen fibres in the deep dermis (DD) revealed greater resistance. The corresponding Elastica–Masson staining sections before and after digestion are displayed at the bottom.

(B) Time course of SOS after pepsin digestion. Average SOS (m/s) and SD of the

epidermis, deep and papillary dermis and skeletal muscles after pepsin digestion. **$P <$ 0.01

Figure 6

Changes in SOS of the aortic valve after pepsin digestion.

Paraffin sections of the aortic valve from a 53-year-old woman (A) and a 74-year-old man (B) were incubated in pepsin solutions for 1 h. Before and after digestion, the sections were observed with SAM. Then, the same sections were more digested up to 3 h. Collagen bundles in the fibrosa layer in A showed a rapid decrease in SOS during this time course compared with B which maintained almost the same SOS. The optical images shown at the bottom correspond to the SAM images before and 3 h after digestion and reveal that the valve structures were well preserved. The graph (C) shows the time course of average SOS (m/s) and SD after pepsin digestion. **$P < 0.01$

Figure 7

SOS change of old and acute myocardial infarction after pepsin digestion.

Paraffin sections of the heart with old (A) or acute (B) infarction were incubated in pepsin solution. The old infarcted area with scar formation showed no changes in SOS,

while the acute infarcted area with bleeding and neutrophillic infiltration revealed a conspicuous decrease in SOS. The corresponding histological sections before and 3 h after digestion are shown at the bottom. The graph (C) shows the time course of the average SOS (m/s) and SD after pepsin digestion. $^{**}P < 0.01$, $^{*}P < 0.05$

Supporting Information

Table S1. SOS of small intestine after formalin fixation

The average SOS (m/s) and SD of the intestinal mucosa after formalin fixation were shown. Fresh frozen sections from three mice were calculated.

SOS, speed of sound; Ave, average; SD, standard deviation

Table S2. Difference of SOS between ethanol and formalin fixation.

The average SOS (m/s) and SD of the oral squamous cells and peripheral white blood cells after ethanol and formalin fixation were shown.

SOS, speed of sound; OSC, oral squamous cells; PB, peripheral white blood cells; EtOH, ethanol; FA, 10% formalin; Ave, average, SD, standard deviation

Table S3. Difference of thickness between ethanol and formalin fixation.

The average thickness (μm) and SD of the oral squamous cells and peripheral white blood cells after ethanol and formalin fixation were shown.

SOS, speed of sound; OSC, oral squamous cells; PB, peripheral white blood cells; EtOH, ethanol; FA, 10% formalin; Ave, average, SD, standard deviation

Table S4. Average SOS (m/s) and SD of FFPE sections after fixation.

The average SOS (m/s) and SD of formalin-fixed, paraffin-embedded (FFPE) tissues in different fixation time, 1 day, 3 days, 1 week, and 3 months are shown.

SOS, speed of sound; SD, standard deviation; FFPE, formalin-fixed, paraffin-embedded; Lg Intestine, large intestine; Kid Cortex, kidney cortex; Kid Medulla, kidney medulla.

Samples were collected from three mice.

Table S5. Average SOS (m/s) and SD of the glomeruli and tubules of normal and diabetic kidneys.

The average SOS (m/s) and SD of normal and diabetic kidney paraffin sections before and after PAS procedure were shown.

SOS, speed of sound; SD, standard deviation; Ave, average; SD, standard deviation; Nor, normal; GM, glomerulus; T-BM, tubular basement membrane; pre, pre-reaction; PAS, post-PAS reaction

Table S6. Average SOS (m/s) and SD of the ulcerated skin after pepsin digestion.

The time course of SOS after pepsin digestion. Average SOS (m/s) and SD of the epidermis, deep and papillary dermis, and skeletal muscles after pepsin digestion were shown.

SOS, speed of sound; SD, standard deviation; MS, skeletal muscle; DD, deep dermis; PD, papillary dermis; EP, epidermis

Table S7. Average SOS (m/s) and SD of the aortic valve (AV) after pepsin digestion.

The time course of average SOS (m/s) and SD after pepsin digestion were shown.

SOS, speed of sound; SD, standard deviation; AV, aortic valve; Ave, average; SD, standard deviation

Table S8. Average SOS (m/s) and SD of the myocardial infarction after pepsin digestion.

The time course of average SOS (m/s) and SD after pepsin digestion were shown.

SOS, speed of sound; SD, standard deviation; AMI, acute myocardial infarction; CMS, cardiac muscle

Fig. 1
A

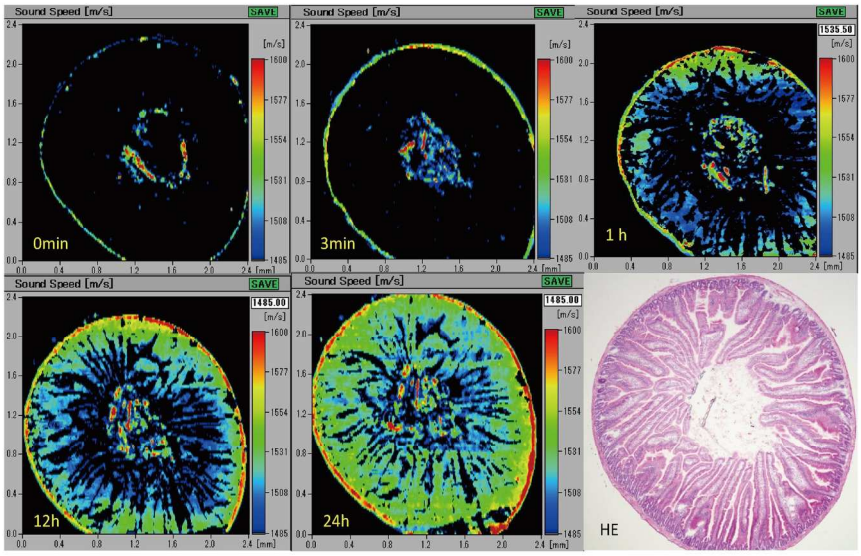

B

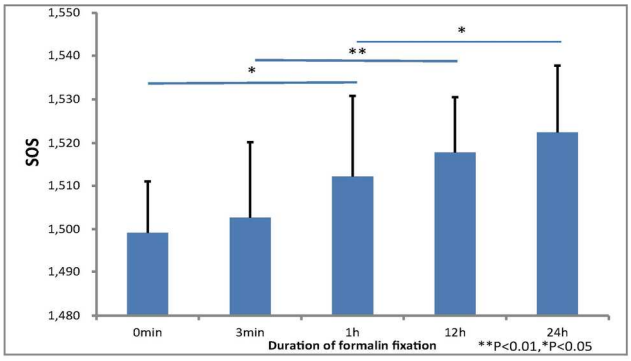

Change in speed of sound after formalin fixation.
(A) A fresh frozen section of mouse small intestine was soaked in 10% buffered formalin for 3 min, washed in distilled water and observed under a scanning acoustic microscope (SAM). The same section was fixed according to the same process, but for varying durations of 1, 12 and 24 h. The values of speed of sound (SOS) increased in accordance with fixation time. The corresponding HE section after 24 h fixation is shown at the lower right.
(B) Average SOS (m/s) and SD of the mucosa after formalin fixation. **P < 0.01, *P < 0.05

161x215mm (300 x 300 DPI)

Fig. 2

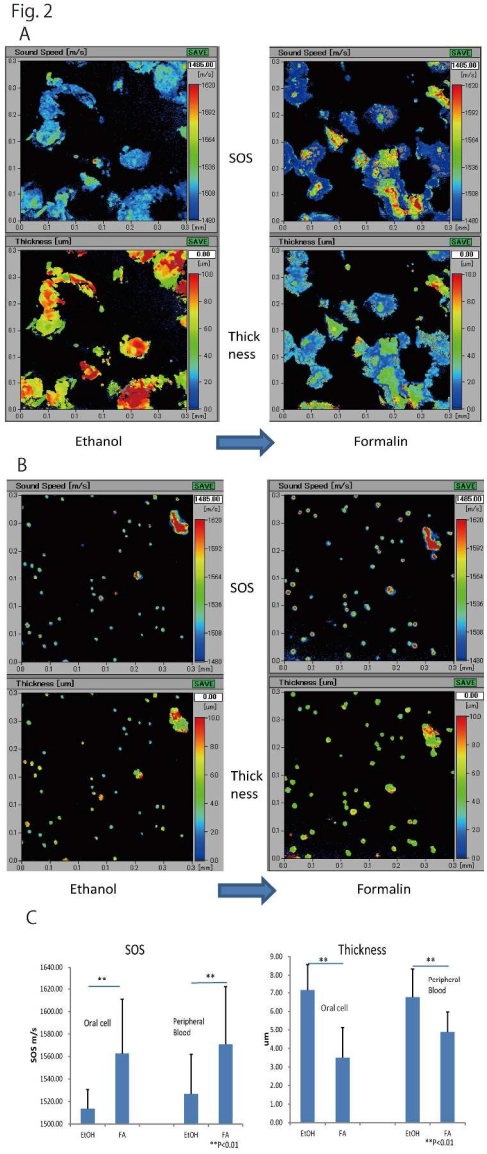

Effects of fixation difference between ethanol and formalin.
Oral squamous cells (A) and peripheral white blood cells (B) were smeared on a glass slide, fixed in ethanol and observed with SAM. The cells were then fixed in 10% formalin. The upper figures indicate the SOS images and the lower figures indicate the thickness of each point. Each left and right image corresponds to almost same area. The graph (C) shows average SOS (m/s) and thickness (μm) with SD. **P < 0.01

287x683mm (300 x 300 DPI)

Fig.3

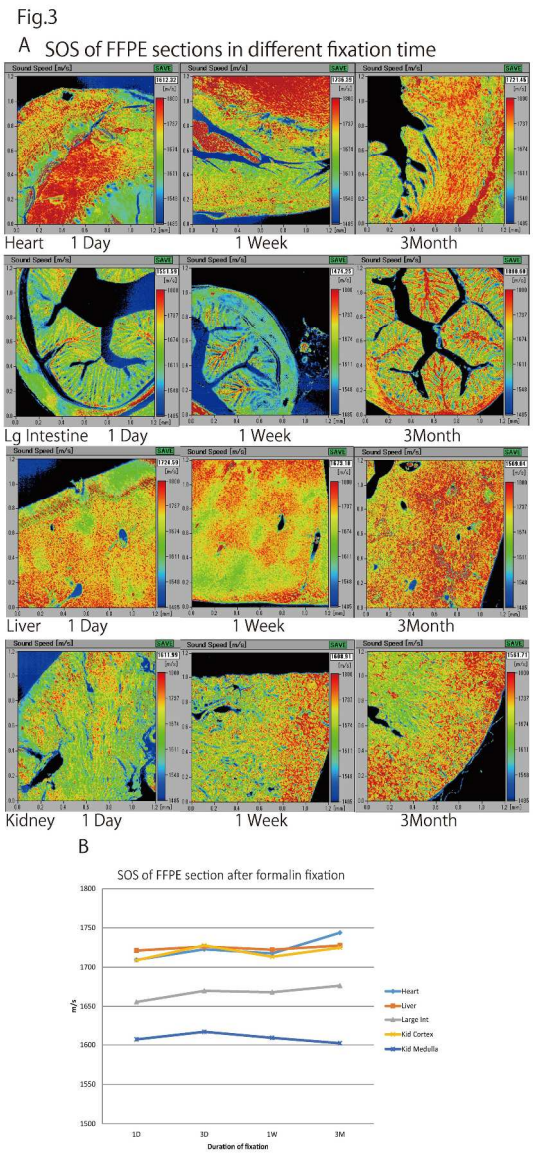

The SOS of formalin-fixed, paraffin-embedded tissues at different fixation times.
(A) Images of SOS of various organs of mice such as heart, large intestines, liver and kidneys in different fixation times of 1 day, 1 week and 3 months are displayed.
(B) Average SOS (m/s) of various formalin-fixed, paraffin-embedded (FFPE) organs at different fixation times.

262x570mm (300 x 300 DPI)

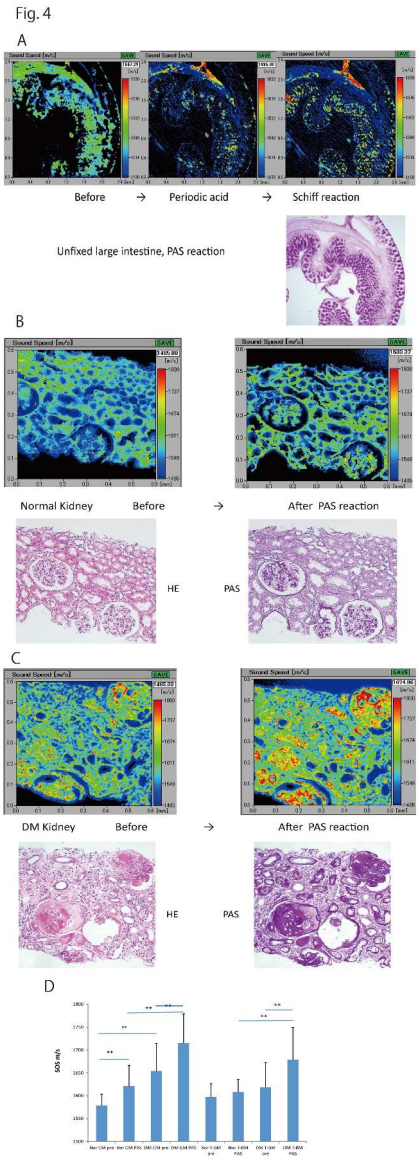

Change in SOS during the periodic acid Schiff procedure.
A fresh frozen section of mouse large intestine (A) was mounted with 1% periodic acid solution for 10 min, washed in distilled water and treated with Schiff reagent for 10 min. The images of SOS (left, before reaction; middle, after periodic acid oxidation; right, after Schiff reagent). The mucus in the goblet cells was pursuable by the increased SOS during the periodic acid Schiff (PAS) procedure. The corresponding light microscopic image after the PAS procedure is present at the lower right corner.
The SOS images of normal (B) and diabetic (C) kidney paraffin sections before and after PAS procedure. The SOS of the glomeruli and tubular basement membranes of the diabetic kidney promptly increased after the Schiff reaction compared with normal kidneys. The corresponding LM images are shown at the lower right corner. The graph (D) shows the average SOS (m/s) and SD of the glomeruli and tubules of normal and diabetic kidneys. Nor, normal; GM, glomerulus; T-BM, tubular basement membrane. **P < 0.01

336x929mm (300 x 300 DPI)

Fig. 5

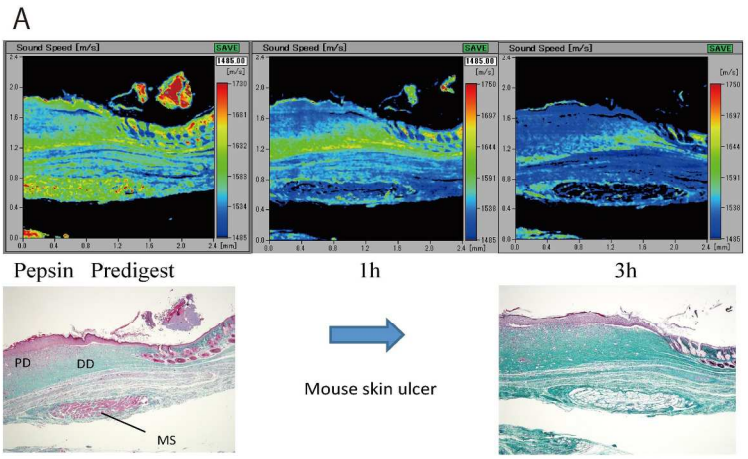

Change in SOS of mouse skin after pepsin digestion.
(A) A paraffin section of ulcerated mouse skin was incubated in pepsin in 10 mM HCl solution. After 1 and 3 h, the same section was observed under SAM. The epidermis, papillary dermis (PD) with granulation tissue and skeletal muscles (MS) displayed prompt reductions in SOS. The keratin fibres, fine collagen fibres and muscle fibres were more sensitive to protease digestion, while the thick collagen fibres in the deep dermis (DD) revealed greater resistance. The corresponding Elastica–Masson staining sections before and after digestion are displayed at the bottom.
(B) Time course of SOS after pepsin digestion. Average SOS (m/s) and SD of the epidermis, deep and papillary dermis and skeletal muscles after pepsin digestion. **P < 0.01

180x270mm (300 x 300 DPI)

Fig. 6

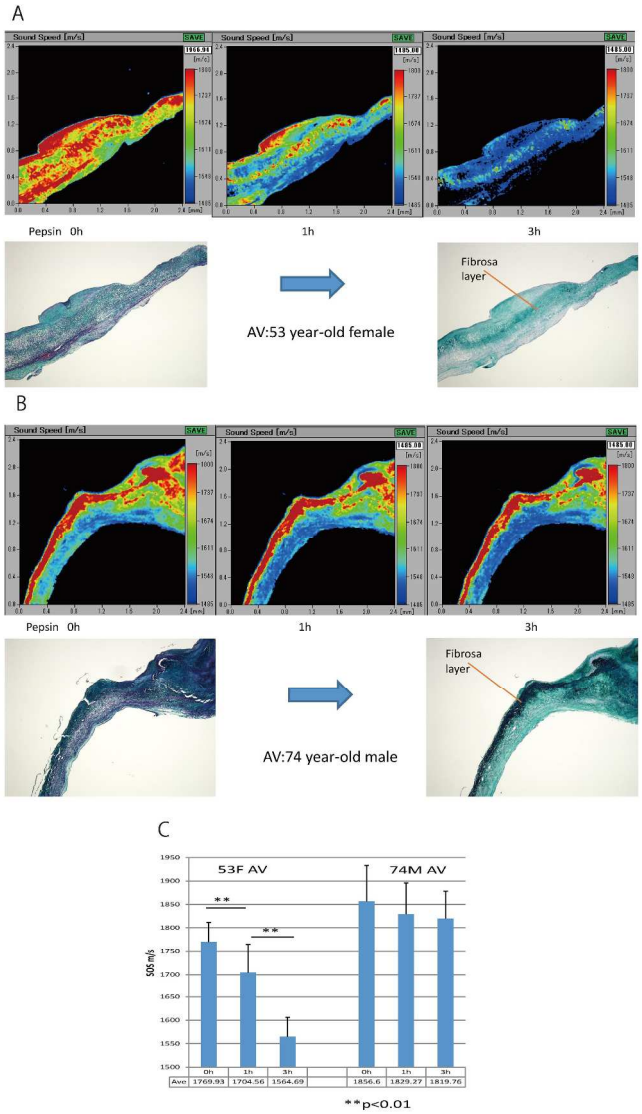

Changes in SOS of the aortic valve after pepsin digestion.
Paraffin sections of the aortic valve from a 53-year-old woman (A) and a 74-year-old man (B) were incubated in pepsin solutions for 1 h. Before and after digestion, the sections were observed with SAM. Then, the same sections were more digested up to 3 h. Collagen bundles in the fibrosa layer in A showed a rapid decrease in SOS during this time course compared with B which maintained almost the same SOS. The optical images shown at the bottom correspond to the SAM images before and 3 h after digestion and reveal that the valve structures were well preserved. The graph (C) shows the time course of average SOS (m/s) and SD after pepsin digestion. **P < 0.01

216x387mm (300 x 300 DPI)

Fig.7

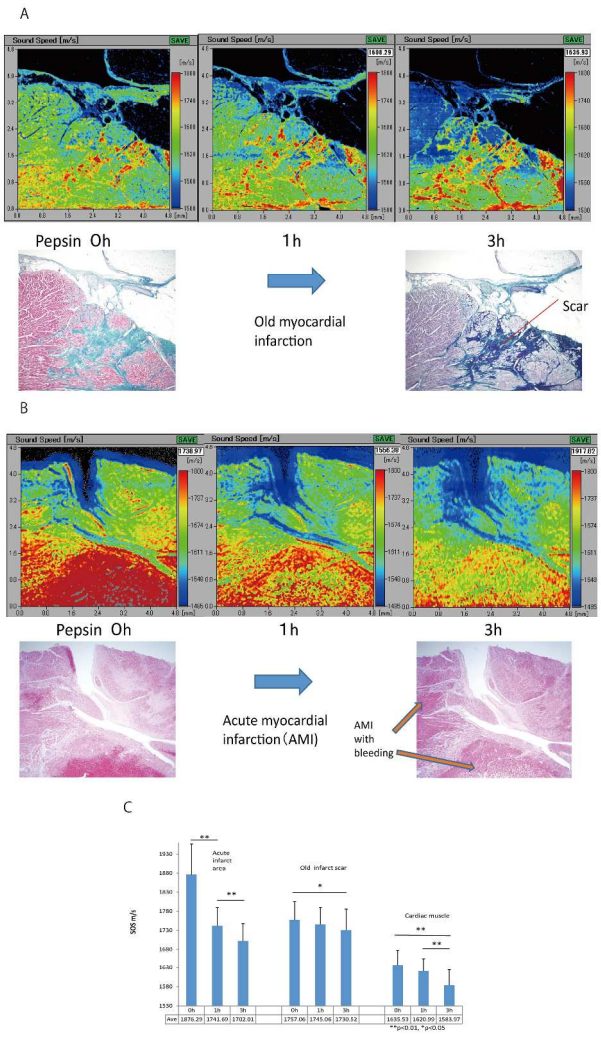

SOS change of old and acute myocardial infarction after pepsin digestion.
Paraffin sections of the heart with old (A) or acute (B) infarction were incubated in pepsin solution. The old infarcted area with scar formation showed no changes in SOS, while the acute infarcted area with bleeding and neutrophillic infiltration revealed a conspicuous decrease in SOS. The corresponding histological sections before and 3 h after digestion are shown at the bottom. The graph (C) shows the time course of the average SOS (m/s) and SD after pepsin digestion. **P < 0.01, *P < 0.05

356x700mm (300 x 300 DPI)

Table S1. SOS of small intestine after formalin fixation

Fixation Time	n	Ave(m/s)	SD(m/s)
0min	21	1499.19	11.78
3min	19	1502.69	17.53
1h	39	1512.09	18.68
12h	34	1517.69	12.78
24h	40	1522.44	15.24

Table S2. Difference of SOS between ethanol and formalin fixation.

	SOS	n	Ave m/s	SD m/s
OSC	EtOH	41	1513.51	17.14
	FA	52	1562.52	48.41
PB	EtOH	50	1526.65	35.24
	FA	68	1570.78	51.22

Table S3. Difference of thickness between ethanol and formalin fixation.

	Thickness	n	μm	SD
OSC	EtOH	41	7.15	1.42
	FA	52	3.5	1.62
PB	EtOH	50	6.76	1.57
	FA	68	4.89	1.08

Table S4. Average SOS (m/s) and SD of FFPE sections after fixation.

Fixation duration	Heart n(60)	Liver n(60)	Lg Intestine n(89)	Kid Cortex n(60)	Kid Medulla n(60)
1D	1709.26±69.18	1721.13±53.26	1655.64±40.10	1708.72±40.10	1606.84±48.26
3D	1722.78±56.12	1726.20±61.44	1669.82±53.67	1727.74±53.67	1616.59±52.79
1W	1717.43±40.39	1722.29±66.44	1668.05±54.05	1713.21±54.05	1608.89±44.73
3M	1743.94±37.34	1727.53±65.30	1676.37±59.89	1724.88±59.89	1602.06±46.63

Table S5. Average SOS (m/s) and SD of the glomeruli and tubules of normal and diabetic kidneys.

Kidney section	n	Ave (m/s)	SD(m/s)
Nor GM pre	60	1578.51	24.66
Nor GM PAS	60	1620.82	45.31
DM GM pre	60	1654.09	60.09
DM GM PAS	60	1715.35	63.08
Nor T-BM pre	60	1597.48	28.84
Nor T-BM PAS	60	1607.82	28.14
DM T-BM pre	60	1618.62	53.42
DM T-BM PAS	60	1678.53	70.98

Table S6. Average SOS (m/s) and SD of the ulcerated skin after pepsin digestion.

	n	Ave	SD
MS			
0h	20	1607.09	38.44
1h	20	1521.54	24.16
3h	20	1512.35	21.62
DD			
0h	20	1621.38	15.56
1h	20	1618.17	24.15
3h	20	1577.08	22.89
PD			
0h	20	1559.40	17.20
1h	20	1537.86	11.15
3h	20	1522.39	10.33
EP			
0h	20	1628.87	38.71
1h	20	1542.01	18.67
3h	20	1506.84	20.24

Table S7. Average SOS (m/s) and SD of the aortic valve (AV) after pepsin digestion.

53F AV	n	Ave	SD
0h	30	1769.93	41.77
1h	30	1704.56	59.69
3h	30	1564.69	41.63
74M AV			
0h	30	1856.60	76.47
1h	30	1829.27	66.59
3h	30	1819.76	58.37

Table S8. Average SOS (m/s) and SD of the myocardial infarction after pepsin digestion.

	Time	n	Ave	SD
AMI	0h	60	1876.29	79.87
	1h	60	1741.69	48.25
	3h	60	1702.01	45.70
Scar	0h	40	1757.06	48.04
	1h	40	1745.06	44.98
	3h	40	1730.52	55.47
CMS	0h	40	1635.53	41.46
	1h	40	1620.99	33.69
	3h	40	1583.97	40.73